Translational Oncology

www.transonc.com

Volume 8 Number 5 October 2015 pp. 358–367 358

# A Preclinical Model of Inflammatory Breast Cancer to Study the Involvement of CXCR4 and ACKR3 in the Metastatic Process

**Roberto Wurth[*,1,2], Kevin Tarn[*,2], Danielle Jernigan[*], Sandra V. Fernandez[‡], Massimo Cristofanilli[‡], Alessandro Fatatis[*,§,#] and Olimpia Meucci[*,**]**

*Department of Pharmacology and Physiology, Drexel University College of Medicine, 245 N. 15th Street, Philadelphia, PA 19102; [†]Department of Medical Oncology, Sidney Kimmel Cancer Center, Thomas Jefferson University, 233 S. 10th Street, Philadelphia, PA 19107; [‡]Department of Pathology and Laboratory Medicine, Drexel University College of Medicine, 245 N. 15th Street, Philadelphia, PA 19012; [§]Biology of Prostate Cancer Program, Sidney Kimmel Cancer Center, Thomas Jefferson University, 233 S. 10th Street, Philadelphia, PA 19107; [¶]Department of Microbiology and Immunology, Drexel University College of Medicine, 245 N. 15th Street, Philadelphia, PA 19102

## Abstract

Inflammatory breast cancer (IBC) is an aggressive and invasive tumor, accounting for 2.5% of all breast cancer cases, and characterized by rapid progression, regional and distant metastases, younger age of onset, and lower overall survival. Presently, there are no effective therapies against IBC and a paucity of model systems. Our aim was to develop a clinically relevant IBC model that would allow investigations on the role of chemokine receptors in IBC metastasis. Primary cultures of tumor cells were isolated from pleural exudates of an IBC patient and grown as spheres or monolayers. We developed a human xenograft model where patient-derived IBC cells, stably transduced with lentiviral vectors expressing fluorescent and bioluminescent markers, were inoculated directly into the left ventricle of mice. Our *in vivo* data show that these IBC cells (FC-IBC02A) are able to seed and proliferate into various organs, including brain, lungs, lymph nodes, and bone, closely replicating the metastatic spread observed in IBC patients. Moreover, cells were able to generate tumors when grafted in the mammary fat pad of mice. RT-PCR and microscopy studies revealed expression of both CXCR4 and ACKR3 receptors in FC-IBC02A cells. Furthermore, CXCL12 (the endogenous chemokine ligand of these receptors) induced transendothelial migration of these cells and stimulated signaling pathways involved in cell survival and migration - an effect reduced by CXCR4 or ACKR3 antagonists. This new model can be used to develop chemokine-based pharmacological approaches against the IBC metastatic process. This work also provides the first evidence of ACKR3 expression in IBC cells.

*Translational Oncology (2015) 8, 358–367*

## Background

Inflammatory breast cancer (IBC) is an aggressive and rare form of invasive breast cancer that presents with very distinct clinical and pathological features [1]. Clinical symptoms of IBC are most frequently associated with acute onset of edema, erythema, and an orange-peel (peau d'orange) appearance of the overlying skin in the

Address all correspondence to: Olimpia Meucci, MD, PhD, Department of Pharmacology and Physiology, Drexel University College of Medicine, 245 North 15th street, NCB 8221, Philadelphia, PA 19102.
E-mail: rowurth@gmail.com

[1] Roberto Wurth's present affiliation: Department of Internal Medicine, University of Genoa, Italy.

[2] Denotes equal contribution.

Received 23 June 2015; Revised 20 July 2015; Accepted 29 July 2015



1936-5233/15
http://dx.doi.org/10.1016/j.tranon.2015.07.002

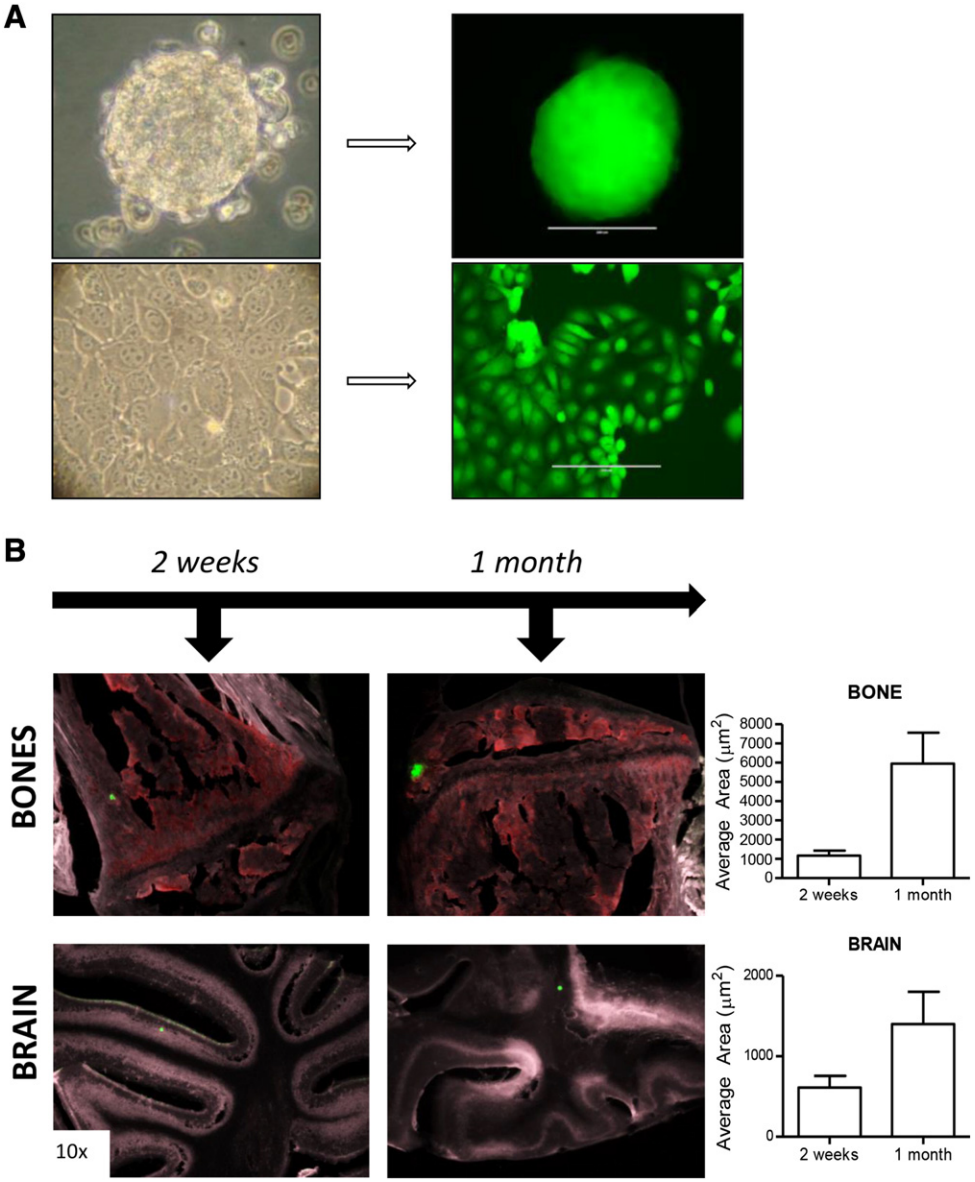


**Figure 1.** In vitro/in vivo model of IBC: (A) Human IBC-cells (FC-IBC02A) were cultured as monolayer or spheres. Sphere-derived and monolayer FC-IBC02A cells were engineered to stably express enhanced Green Fluorescent Protein (eGFP) as detailed in the methods. (B) Sphere-derived cells and monolayer eGFP-FC-IBC02A cells were both able to spread to and proliferate in brain and bones (250,000 cells were injected intracardially). For bones: cells were consistently detected along the growth plate in femora and tibiae. Longer term *in vivo* studies (2 and 4 weeks) showed the proliferative capability of disseminated IBC-cells. N = 3 animals (4 foci); data shown as mean ± SEM.

affected breast. As the majority of patients do not present with a discrete palpable mass, IBC is often misdiagnosed upon clinical examination [1]. Furthermore, due to the invasion of tumor cell aggregates into lymphatic channels, IBC presents peculiar features that can mimic an acute inflammation [2]. Although it is estimated that IBC accounts for about 2.5% of all breast cancer cases in the United States, patients diagnosed with IBC have the worst prognoses and continue to have poorer survival outcomes compared with patients with other variants of the disease [3,4]. Even with the addition of multimodal therapies consisting of neo-adjuvant chemotherapy followed by surgery and radiotherapy, 5-year overall survival rates reach at best 25-28% [5,6]. This is in part due to IBC's high metastatic potential and propensity to invade blood vessels [2]. IBC patients have shown a disposition to develop metastases in the brain, bones, and various visceral organs [5].

There is increasing evidence that the expression of select chemokine receptors play an important role in breast cancer metastasis and prognosis [7–11]. Among them, the G protein-coupled receptor CXCR4 and its activating ligand CXCL12 (also known as stromal derived factor-1α) have been shown to be overexpressed in over 20 different tumor types [12]. Furthermore, enhanced expression of CXCR4 has been directly correlated with poor overall survival in metastatic breast carcinomas [13]. The recently identified chemokine receptor ACKR3, formerly known as CXCR7, also plays a role in CXCL12/CXCR4 signaling [14]. This atypical chemokine receptor can act as a CXCL12 scavenger, signal

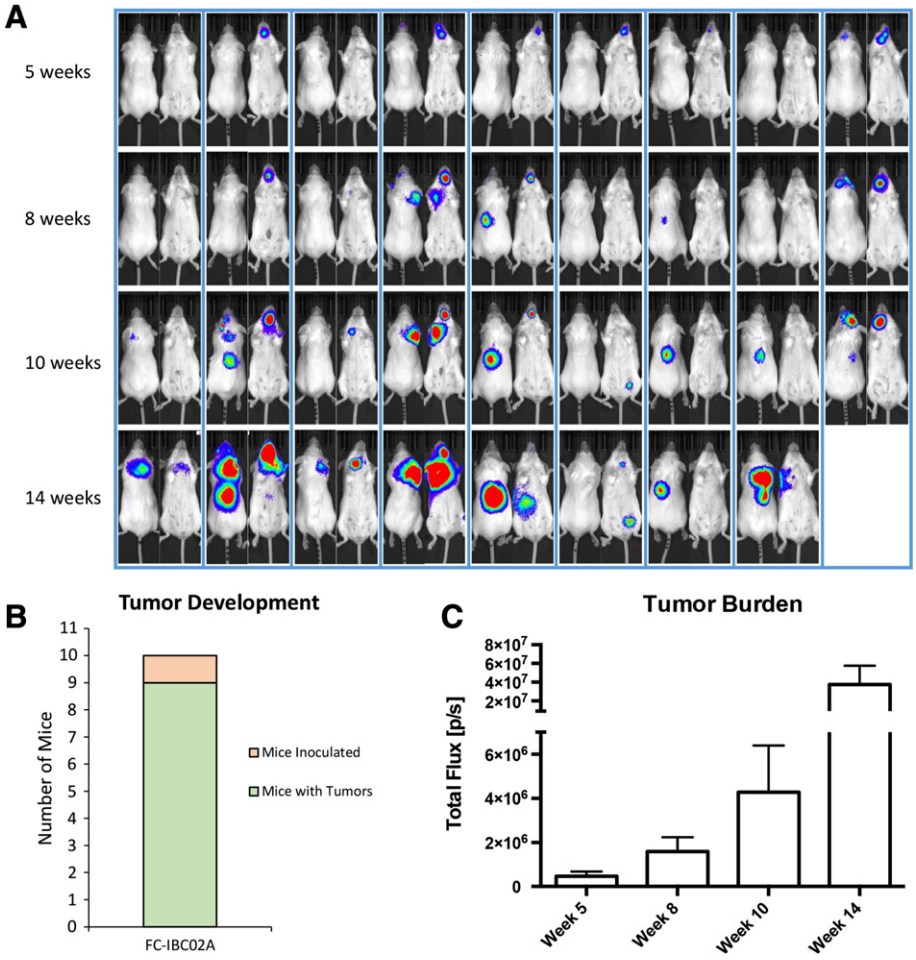


**Figure 2.** In vivo bioluminescence model: (A) Tumors development *in vivo* was followed by bioluminescence over a course of 14 weeks. The eGFP-luciferase cell line was obtained by infecting eGFP-FC-IBC02A cells with a Red Firefly Luciferase expressing lentivirus; 250,000 cells were injected intracardially. (B) Nine out of ten mice inoculated with FC-IBC02A cells developed tumors. (C) Total tumor burden was quantified using Living Image Software (Caliper Life Sciences) and data are shown as mean ± SEM (total flux [p/s]). N = 9 animals. Graphs in B/C include data from various organs.

via the arrestin pathway, and/or modulate CXCR4-mediated responses through direct or indirect interactions [15–17]. The downstream pathways of CXCR4 are important for the proliferation, survival, and migration of cancer cells [12,18]. Tumor cells that overexpress CXCR4 co-opt the chemokine system normally used by leukocyte trafficking in order to migrate to organs that secrete high concentrations of CXCL12 such as the brain, lungs, liver, and bone marrow. CXCR4 also facilitates primary tumor growth through promoting angiogenesis via up-regulation of VEGF and recruitment of endothelial progenitor cells [12]. Considering the impact of metastasis in the overall survival of IBC patients, a better understanding of the metastatic process is essential to develop effective therapeutic strategies. Thus, preclinical models that predict patient response, mimic complex and tissue-specific patterns of metastasis, and enable early accurate detection of secondary lesions are greatly needed. To this end, using a cell line obtained from the pleural exudate of an IBC patient, we recently developed a preliminary in vivo model of IBC [19]. Here, we present a refined version of this model that allows study of early as well late stage IBC metastases and of the involvement of CXCR4/ACKR3 in this process. Our approach introduces a visual advantage in identifying individual disseminated tumor cells (DTCs) of IBC origin with the use of fluorescent labeling, thus allowing investigations on the early stages of the in vivo dissemination process driven by these cells. Long-term monitoring of tumor progression is afforded by the simultaneous expression of the luciferase gene. We also characterized expression and function of critical chemokine receptors in the IBC cells. Overall, our data suggest that these cells are an excellent tool for both in vitro and in vivo investigations concerning the roles of the CXCL12-CXCR4/ACKR3 axis in IBC migration, growth, and invasion.

## Materials and Methods

### *Cell Cultures*

Human primary IBC cells (FC-IBC02A) were isolated from the pleural exudate of an IBC patient and cultured as monolayer or mammospheres. The patient had signed an informed consent from the Fox Chase Cancer Center (FCCC) Human Subject Protection Committee prior to sample collection. Both the Research Review Committee (RRC) and the Institutional Review Board (IRB) at FCCC approved the study (approval #10-826). Cells in monolayer were grown in DMEM containing 10% fetal bovine serum (Hyclone, Logan, UT, USA) and 0.1% gentamicin (Invitrogen, Carlsbad, CA) and kept at 37°C and 5% $CO_2$. Spheres were grown in suspension

**Table 1.** Metastatic spread of FC-IBC02A via intracardiac injection route.

| Tumor Location | Mouse1 | Mouse2 | Mouse3 | Mouse4 | Mouse5 | Mouse6 | Mouse7 | Mouse8 | Mouse9 | Mouse10 * |
|---|---|---|---|---|---|---|---|---|---|---|
| Brain | - | - | - | - | - | - | 1 | - | - | - |
| Knee joint | - | - | - | 1 | - | - | - | - | - | 1 |
| Lymph node | 1 | - | 1 | 1 | 1 | - | - | - | 1 | - |
| Adrenal gland | - | - | 1 | - | - | 1 | - | 1 | 1 | - |

* This animal was sacrificed at 10 weeks.

using a proliferation permissive serum-free medium (Mammary Epithelial Cell Growth Medium, MEGM) containing: Mammary Epithelial Cell Basal Medium (MEBM), 2% B27 supplement, heparin (4 μg/ml), recombinant human bFGF (20 ng/ml), and EGF (20 ng/ml), and an antibiotics-antimycotic solution composed of Streptomycin, Amphotericin B, and Penicillin (Gibco, 15240, Grand Island, NY). FC-IBC02A cells were stably transduced with lentiviral vectors expressing constitutive eGFP (Lentivector: pHRCMVO2-EFtet from AmeriPharma) [20] and luciferase, produced by subcloning the Red Firefly Luciferase gene (from pMCS-Red Firefly Luc; Thermo Fisher Scientific, Waltham, MA) into the BamH1 and Xho1 sites of pENTR1A no ccDB (Addgene, Cambridge, MA) then transferred via Gateway LR Clonase II (Thermo Fisher) into pLenti CMV puro DEST (Addgene) these cells were used for both *in vitro* and *in vivo* experiments. FC-IBC02A cells were authenticated for human origin and gender by IDEXX Laboratories, Columbia, MO (case number: 18505-2012).

Primary human brain microvascular endothelial cells (HBMECs) were purchased from ScienCell (Carlsbad, CA). HBMEC were grown in Endothelial cell medium (ECM, ScienCell) in tissue culture flasks coated with Fibronectin (Cell Systems). Cells were passaged according to the manufacturer's instructions and used up to passage eight.

### *Immunocytochemistry*

Monolayer cells on coverslips and spheres on chamber slides were fixed in 4% paraformaldehyde. Cells were then permeabilized with 0.1% Triton X-100 for 5 minutes. The following antibodies were used: mouse anti-ACKR3 (clone 11G8; 50 mg/mL—a gift from ChemoCentryx), mouse anti-CXCR4 (clone 12G5; 1:200—R&D Systems, Minneapolis, MN). Confocal images were captured with a Zeiss LSM5 Exciter laser scanning confocal microscope (Thornwood, NY) using sequential imaging to prevent interchannel cross-excitation between fluorochromes.

### *RT-PCR*

Total RNA was extracted using the RNeasy mini kit (Qiagen, Valencia, CA). RNA obtained from human cells was treated with DNase prior to RT reaction.

cDNA was synthesized from total RNA. The following primers were used for amplification. *CXCR4*: 5′-GGCCCTCAAGACCA CAGTCA-3′ and 5′-TTAGCTGGAGTGAAAACTTGAAG-3′; *ACKR3*: 5′-ACGTGGTGGTCTTCCTTGTC-3′ and 5′-AAGGC CTTCATCAGCTCGTA-3′; *CXCL12*: 5′-ATGAACGCCAA GGTCGTGGTC-3′ and 5′-CTTGTTTAAAGCTTTCTCCAGG TACT-3′; *human 28S*: 5′-GTTCACCCA CTAATAGGGAA CGTGA- 3′ and 5′-GGATTCTGACTTAGA GGCGTTCAGT-3′. PCR was performed as follows: 5 minutes at 94°C, 35 cycles of 30 s at 94°C, 30 s at 60°C, and 30 s at 72°C, followed by 7 min at 72°C. For gel electrophoresis analysis, each amplicon was generated and visualized using ethidium bromide staining after electrophoresis on a 1.8 % agarose gel. Human 28S was used as loading control.

### *Western Blot*

Cells were washed with ice-cold balanced salt solution and scraped in lysis buffer (50 mM Tris, 150 mM NaCl, 0.5% sodium deoxycholate, 0.1% sodium dodecyl sulfate [SDS], 10 mM Na4P2O7, 5 mM ethylenediaminetetra-acetic acid [EDTA], 1% Triton X-100, 1 mM dithiothreitol, with protease (Calbiochem, cat#539134) and phosphatase (Calbiochem, cat#524625) inhibitor cocktails). Equal amounts of proteins as determined by the bicinchoninic acid assay from Thermo Scientific (Rockford, IL) were loaded in each lane, separated by sodium dodecyl sulfate–polyacrylamide gel electrophoresis (SDS-PAGE), and transferred to polyvinylidene fluoride membranes for immunoblotting. The following primary antibodies were used: anti-pERK1/2 (1:1000, cat#9101, Cell Signaling, Danvers, MA), anti-ERK1/2 (1:1000, cat#9102, Cell Signaling). Anti-actin was used for loading control (1:5000, Sigma-Aldrich).

### *Transendothelial Migration*

Transendothelial migration of FC-IBC02A cells was performed using HTS FluoroBlok 8.0 μm colored PET Membrane Inserts for 24-well plates (BD Falcon). 50,000 HBMECs were added to fibronectin-coated 24-well (overnight coating) inserts and grown for at least 5 days in 5% $CO_2$ at 37°C. The medium was replaced every day with fresh medium. Before cell migration assays were performed, the integrity of the cell monolayer was confirmed by monitoring of Trans-endothelial electrical resistance (TEER), measured with an Epithelial Voltohmmeter (EVOM, World Precision Instruments). To obtain TEER values in $\Omega \times cm^2$, the mean resistance of an empty insert was subtracted from the mean resistance of the insert with cultured cells (3 readings per insert). This value was then multiplied by the surface area of the insert (0.33 $cm^2$). eGFP-FC-IBC02A cells ($2\times10^5$) in 1% FBS, 0.1% BSA DMEM were seeded in the upper chamber, and 1% FBS, 0.1% BSA DMEM supplemented with 20 nM CXCL12 was applied in the lower chamber. After 8 and 24 hours, transmigrated cells were detected and counted using a digital inverted fluorescence microscope (Evos, AMG, Bothell, WA). For each insert, the entire surface area was counted.

### *In Vivo Tumorigenicity*

To test the ability of monolayer and sphere-derived FC-IBC02A cells to initiate tumor *in vivo*, monolayer ($1\times10^6$) or sphere ($1\times10^5$) dissociated FC-IBC02A cells were resuspended in 100 μL of DMEM/F12 + 100 μL of matrigel (BD Biosciences) and injected into the mammary fat pad of 6–8 weeks old female immunocompromised (CB17-SCRF) mice under anesthesia (ketamine 80 mg/kg and xylazine 10 mg/kg). CB17-SCRF mice were obtained from Taconic (Germantown, NY, USA) and housed in a germ-free barrier. Mice were monitored for disease symptoms and were sacrificed by $CO_2$ asphyxiation when they showed weight loss or any severe sign of disease (8-10 days post injections). Tumors were removed, fixed in formalin, paraffin-embedded, and then stained with hematoxylin-eosin (H&E) for histopathology (n = 3 for each condition).

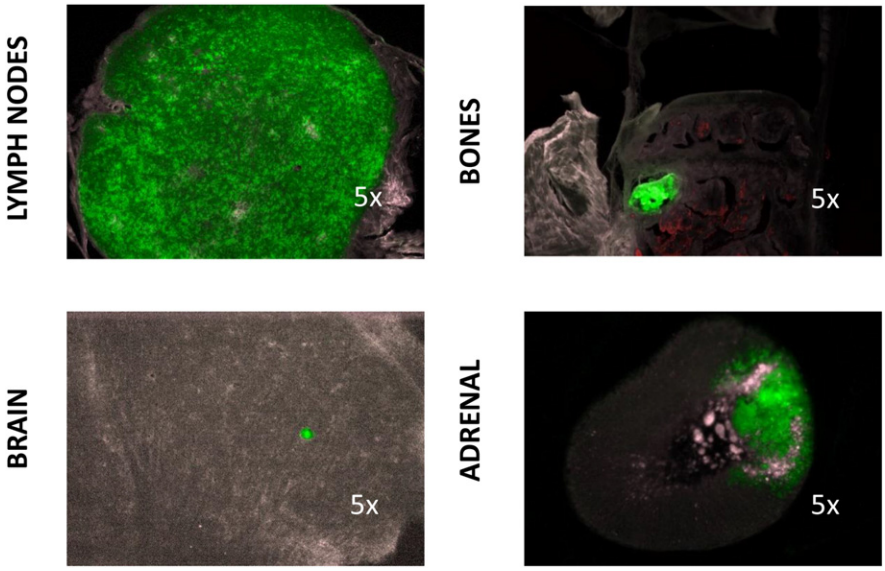


**Figure 3.** Dissemination of FC-IBC02A cells in different organs: Mice were sacrificed after 14 weeks and tissue sections of various organs were obtained as described in the methods. Tumors were found in the brain, adrenal glands, bones, and lymph nodes. Representative fluorescent images of tissue sections confirm the presence of FC-IBC02A *in vivo*.

### *Animal Model of Metastasis*

CB17-SCRF female mice were anesthetized as indicated above and then inoculated in the left cardiac ventricle with either monolayer or sphere-derived human IBC-cells, as we previously described for other cell types [21]. Briefly, cell inoculation was performed using an insulin syringe with a 30-gauge needle. The correct execution of intracardiac inoculation was established by the appearance of fresh arterial blood in the Luer-Lok fitting of the hypodermic needle, which indicated the successful penetration of the ventricular wall. In addition, blue fluorescent polystyrene beads (10 μm diameter, Invitrogen-Molecular Probes) were co-injected with cancer cells. Their detection by fluorescence microscopy in different organs at necropsy confirmed the successful inoculation in the blood circulation. We used 250,000 cells in a total volume of 100 μL of DMEM/F12. Dissemination of cancer cells to the brain, bones and other organs was studied at 10 minutes, 2 weeks, 1 month, and then up to 14 weeks post inoculation. All experiments were performed in accordance with NIH guidelines for the humane use of animals. All protocols involving the use of animals were approved by the Drexel University College of Medicine Committee for the Use and Care of Animals.

### *Tissue Preparation and Cancer Cell Detection*

Continuous long-term *in vivo* monitoring of bioluminescence was performed using the IVIS Lumina XR (PerkinElmer, Waltham, MA). Mice were administered weekly via i.p. with D-Luciferin, K+ Salt Bioluminescent Substrate (PerkinElmer, Waltham, MA) and analysis was completed using Caliper Life Science's Living Image software. Animals were sacrificed and tissues were fixed, decalcified in 0.5 M EDTA if necessary and frozen in O.C.T. embedding medium (Electron Microscopy Sciences, Hatfield, PA, USA). Serial tissue sections of 80 μm in thickness were obtained using a Microm HM550 cryostat (Mikron, San Marcos, CA). Sections of each soft-tissue organs and hind legs were transferred on glass slides, stored at −20°C and examined for cancer cells using a Zeiss AX70 microscope (Carl Zeiss, Oberkochen, Germany) connected to a Nuance Multispectral Imaging System (CRI, Guelph, ON). Digital images were analyzed and processed with the Nuance Software (v. 2.4). Microscope and software calibration for size measurement was regularly performed using a TS-M2 stage micrometer (Oplenic Optronics). Bright field and fluorescence images were acquired with an Olympus DT70 CCD color camera.

### *Statistical Analysis*

Statistical significance was calculated using two-tailed t test or one-way ANOVA. All data are reported as the mean ± SEM. A $P$ value of ≤ .05 was considered statistically significant.

## Results and Discussion

### *Stem Cell Properties and Metastatic Behavior of Cultured IBC Cells*

Human primary IBC cells (FC-IBC02A) were isolated from the pleural exudate of an IBC patient, as previously reported [19], and engineered to stably express green fluorescence protein (GFP) using a lentiviral vector (Figure 1*A*). Cells were cultured as either monolayer or mammospheres. Both types of cultures expressed E-cadherin, an adhesion protein particularly abundant in invasive IBC cells and critical to its invasive and metastatic phenotype [1,22]—these data are reported in panel A of the Supplementary Figure 1. E-Cadherin overexpression in IBC cell types is known to be essential for its metastatic phenotype and its ability to form tumor emboli [23,24]. Normally, a loss of E-cadherin has been shown to promote cell invasiveness and be a fundamental event in the epithelial-mesenchymal transition, however, there is evidence to suggest that this loss of epithelial morphology is not a requirement for the invasion and metastasis of various carcinomas [25]. The expression of E-cadherin in monolayer and sphere-derived FC-IBC02A cells may fall in this paradigm.

We also evaluated the expression of CD44, a cancer stem cell marker. Monolayer-derived cells showed a weak to absent expression of CD44, which was strongly expressed in the spheres (Supplementary Figure 1*A*). However, IBC monolayers cells were able to transition to the sphere form upon the addition of MEGM (Supplementary Figure 1*B*)—suggesting that they retain stem cell potential. Clinically, this may be

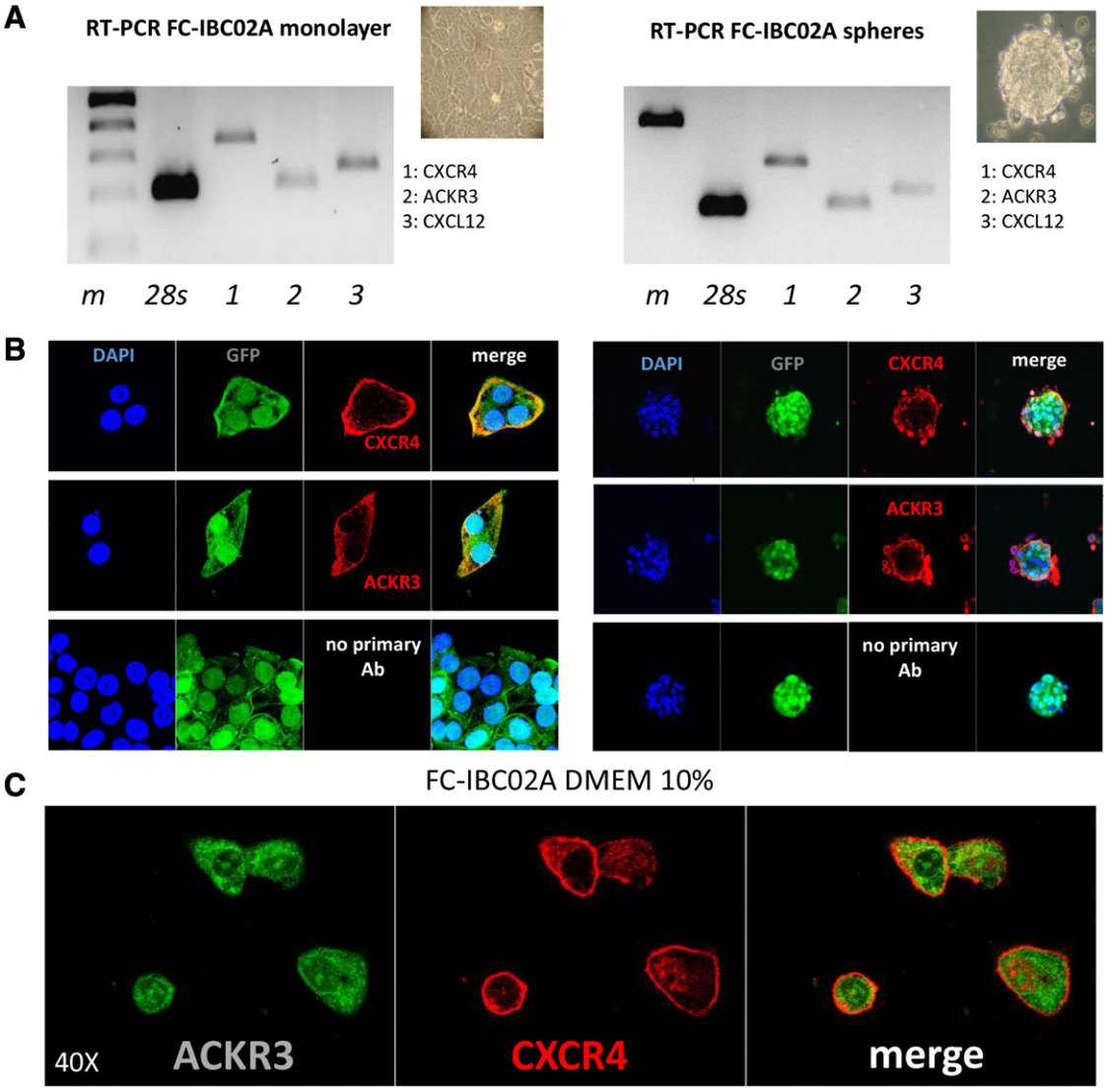


**Figure 4.** Expression of CXCR4 and ACKR3 in FC-IBC02A cells: (A) Reverse-Transcription PCR analysis showing the mRNA expression of the chemokine receptors CXCR4 and ACKR3 and their ligand CXCL12 in FC-IBC02A cells in monolayer (*left*) and spheres (*right*). (B) Representative confocal microscopy micrographs of eGFP-FC-IBC02A-cells in monolayers (*left*) and spheres (*right*). Cells expressed CXCR4 (mouse monoclonal antibody, clone 12G5, red, *top*) and ACKR3 (mouse monoclonal antibody, clone 11G8, green, *middle*). A negative control without primary antibodies is shown (*bottom*). (C) CXCR4 appeared to be localized predominantly to the cellular membrane, while ACKR3 displayed a marked expression in the cytoplasm. Combined merge image show areas of CXCR4 and ACKR3 co-localization. Results are from two independent experiments.

related to the mechanisms of IBC recurrence and dissemination [26,27]. In line with this observation, *in vivo* experiments showed the development of tumors after injection of either monolayer ($10^6$ cells) or dissociated spheres ($10^5$ cells) into the mammary fat pad of 6 to 8 week-old female mice (Supplementary Figure 2*A*). Other studies have also suggested that $CD44^+/CD24^-$/low breast cancer cells exhibit a greater tendency to generate distant metastases [28,29]. Therefore, this transition from $CD44^-$ to $CD44^+$ may also play an active role in FC-IBC02A's ability to invade. In any case, as the two cellular models share similar in vivo properties, this defining feature may facilitate follow-up studies as cells can be rapidly converted from spheres to monolayer and back.

To assess their metastatic potential, we delivered IBC cells directly into the arterial blood circulation via the left cardiac ventricle. The delivery of cancer cells via this route generates circulating tumor cells that rapidly disseminate to skeletal and soft-tissues, closely replicating the distant spreading of primary solid tumors in humans [30]. Tumor cells, cultured as a monolayer, disseminated to areas of known CXCL12 abundance [31,32], including the brain, bones, (Figure 1*B*), lymph nodes, adrenal glands and the lungs (not shown). Ten minutes after the inoculation of FC-IBC02A cells, DTCs were detected along the growth plates of the distal femur, proximal tibia, and brain tissue (Supplementary Figure 2*B*). Longer term *in vivo* studies (2 and 4 weeks) were completed to determine the survival and proliferative potential of disseminated IBC cells in these secondary locations. Tumor foci measuring 1167.68 $\mu m^2$ (± 265.49, n = 4) and 5948.68 $\mu m^2$ (± 1616.78, n = 4), respectively, were observed in the bone at 2 and 4 weeks post-inoculation (Figure 1*B*). A similar pattern of dissemination and colonization was found in the brain, where DTC lesions reached an average size of 1400.23 $\mu m^2$ (± 400.65, n = 5) at 4 weeks. Similar results were obtained using sphere-derived FC-IBC02A cells (not shown).

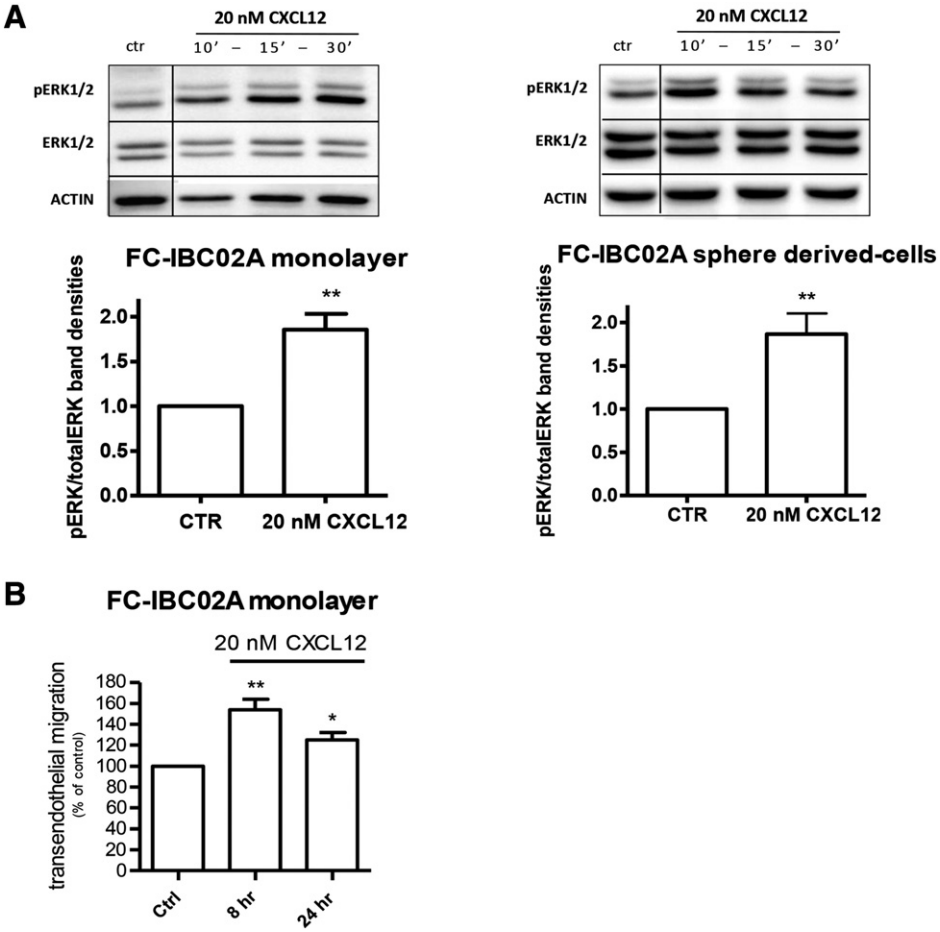


**Figure 5.** Stimulation of CXCR4 and ACKR3 in FC-IBC02A cells—(A) *CXCL12-induced ERK1/2 phosphorylation*. Cell lysates from untreated cultures (ctr) or cultures treated with 20 nM CXCL12 for different times were collected and analyzed by electrophoresis followed by Western blotting. Blots were probed with anti–phospho-ERK1/2 (top panels), by anti–ERK1/2 (middle panel) and anti-actin antibodies (bottom panels) as a loading control. Densitometric analysis showed significant differences in pERK bands after CXCL12 treatment (peak at 15′ for monolayer cells, 10′ for sphere-derived cells) compared with control. Total ERK was used for normalization of pERK. Data represent the mean ± SEM, as obtained in at least three independent experiments. (B) *CXCL12-induced transendothelial migration.* After 8 and 24 hours of exposure to 20 nM CXCL12, transmigrated cells were detected and counted by digital inverted fluorescence microscopy. N = 5, $*P < .05$, $**P < .01$, $***P < .001$.

Continuous long-term *in vivo* studies were performed over the course of 14 weeks using FC-IBC02A cells expressing both luciferase and GFP, as indicated in the methods. Bioluminescence was first detected at 5 weeks, measured by total flux, and monitored weekly over the whole course of the study (Figure 2*A*). One mouse was sacrificed early, at week 10, and thus there is no data available for this animal at week 14. However, in total, nine of ten mice developed bioluminescent signal and were found positive for lesions via tissue sectioning (Figure 2*B*). By using *in vivo* bioluminescence imaging, individual lesions were followed longitudinally. Total flux per animal is normalized and shown in Figure 2*C*. Average tumor burden of each animal at 5 weeks was measured to be 4.601e+05 (± 2.12e+05, n = 9) [photons/second], at 8 weeks total flux was at 1.585e+06 (± 6.52e+05, n = 9) [p/s], at 10 weeks measured at 4.278e+06 (± 2.11e+06, n = 9) [p/s], and at 14 weeks it was measured to be 3.737e+07 (± 2.01e+07, n = 9) [p/s].

At the end of the observation period, animals were sacrificed and dissection was guided by bioluminescence results; tissues were fixed in 4% paraformaldehyde and sectioned. Using fluorescence, bioluminescent signals were confirmed for lesions in the lymph nodes, brain, knee-joints, and adrenal glands (Table 1). Multispectral imaging analysis allowed for GFP labeled FC-IBC02A cells to be discretely isolated from background noise and tumor size accurately measured (Figure 3).

### *Expression of Functional CXCR4 and ACKR3 in IBC Cells*

Previous studies suggested key roles of CXCR4 and ACKR3 in breast cancer progression and metastasis [33,34]. Therefore, it was important to investigate expression of these chemokine receptors in the FC-IBC02A cells. RT-PCR studies showed presence of both CXCR4 and ACKR3 transcripts in these cells (Figure 4*A*). The cells also expressed their chemokine ligand, CXCL12, indicative of possible autocrine/paracrine signaling.

To gain further insight into the cellular localization of the CXCR4 and ACKR3 proteins in the FC-IBC02A cells, immunocytochemistry and confocal microscopy were used. CXCR4 is recognized as the main signaling receptor mediating the biological actions of its only chemokine ligand, CXCL12, whereas ACKR3 primarily acts as a scavenger receptor and regulator of CXCR4 function [35,36]. As shown in Figure 4*B*, under basal conditions, CXCR4 staining was predominantly localized to the cell membrane while ACKR3 was expressed more diffusely, i.e. both at plasma membrane level and in the cytoplasm. Additionally, the ACKR3/

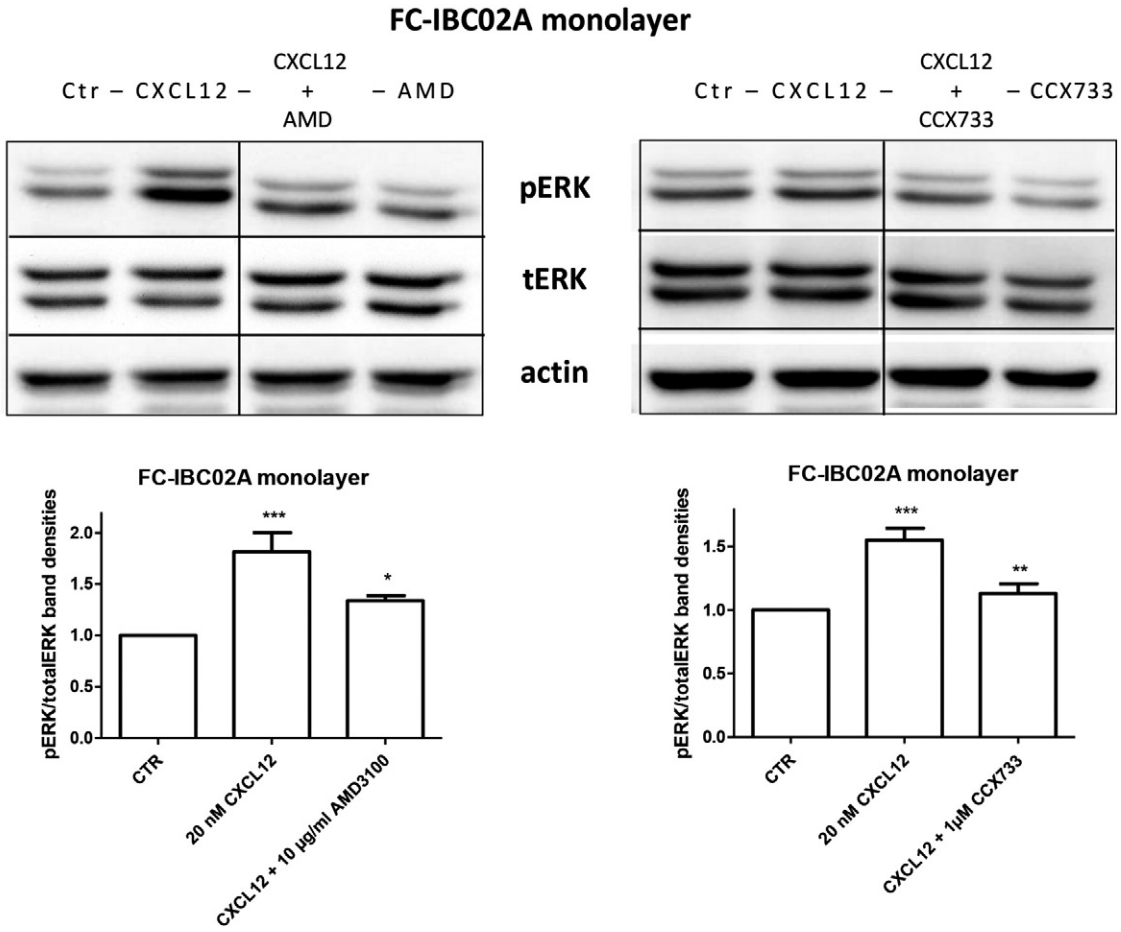


**Figure 6.** CXCL12-induced ERK1/2 phosphorylation is reduced by inhibition of CXCR4 and ACKR3. FC-IBC02A IBC-cells were treated with the CXCR4 inhibitor AMD3100 (10 $\mu$g/mL) or the ACKR3 ligand CCX733 (1 $\mu$M) 15 minutes before (and during) their exposure to vehicle or CXCL12 (20 nM, as indicated). Densitometric analysis showed a reduction in pERK bands after AMD3100 or CCX733 treatment compared with CXCL12 alone. Total ERK was used for normalization of pERK. Data represent the mean ± SEM, as obtained in three or more independent experiments. Images are representative of the same experiment. *$P < .05$, **$P < .01$, ***$P < .001$.

CXCR4 overlay was mainly found in the cytosol, suggesting intracellular associations between the two receptors (Figure 4*C*) and consistent with previous studies, from our group and others, supporting CXCR4/ACKR3 cellular interactions [16,35].

To confirm function of the chemokine receptors in the FC-IBC02A cells, we measured the activation of a typical signaling pathway downstream of CXCR4, i.e., the extracellular regulated kinases 1/2 (ERK1/2). Cell lysates from FC-IBC02A cultures treated with CXCL12 (20 nM)—or vehicle (0.1% BSA/PBS)—were analyzed by Western blot, using antibodies that selectively recognize the total or phosphorylated form of ERK1/2 proteins. As indicated in Figure 5*A*, quantitative analysis showed significant increases of phospho-ERK1/2 after exposure (10, 15, or 30 minutes) of either monolayer or sphere-derived cells to CXCL12, confirming stimulation of CXCR4 in these cells regardless of culture conditions. Next, we evaluated the ability of CXCL12 to stimulate migration of FC-IBC02A cells. To simulate *in vivo* conditions, a transendothelial migration assay was performed using HBMECs as described in the methods. FC-IBC02A cells were plated on one side of a transwell and CXCL12 (20 nM) was added to the other. An increase in the number of transmigrated cells was seen at both 8 and 24 hours (Figure 5*B*) in the presence of CXCL12. Overall, these findings are consistent with the observed CXCR4 expression and the previous reports regarding CXCL12-induced signaling [37].

### *Antagonists of CXCR4 and ACKR3 Inhibit CXCL12 Signaling in IBC Cells*

We next investigated whether treatment with specific chemokine receptor antagonists would inhibit the intracellular signaling pathways stimulated by CXCL12. Thus, prior to exposure of cells to CXCL12, they were treated for 15 minutes with AMD3100 (CXCR4 antagonist) or CCX733 (ACKR3 antagonist) [38,39]. Our data show a marked decrease in ERK1/2 activation in cells co-treated with AMD3100 and CXCL12 (20 µM). Pre-treatment with CCX733 (1 µM) also decreased ERK activation (Figure 6). Thus, similarly to other cell types, CXCR4 and ACKR3 are both involved in CXCL12-induced responses in FC-IBC02A cells.

## Conclusion

In summary, the *in vitro* and *in vivo* data presented here show that FC-IBC02A cells represent an excellent, clinically relevant model to characterize the role of chemokine receptors in the IBC metastatic process. Importantly, FC-IBC02A secondary lesions detected in our pre-clinical model replicate patterns of distant dissemination observed

in IBC patients as shown by axillary lymph node involvement, brain, and bone metastases. The genomic profile of these cells [19] aligns well with their metastatic behavior.

The combined bioluminescence/fluorescence approach described here provides an advantage for longitudinal tracking of individual tumor development that can also serve as a guide during tissue dissection. At the same time, the high sensitivity of advanced multispectral image analysis allows detection of microscopic lesions (made of isolated cells or clusters of few cells), which is instrumental to identification of therapeutic approaches that can interfere with critical steps involved in arrival and survival of circulating tumor cells into the metastatic niche.

Metastatic dissemination of solid tumors is thought to depend on expression of chemokine receptors [7,40]. Although CXCR4 and ACKR3, which are known to regulate cell migration and survival, have been previously implicated in various forms of cancer [41–43], there is very limited knowledge of the involvement of these receptors in IBC, due to the rarity of the disease and the paucity of cellular models available. This work describes an accurate, systematic model to study IBC progression and the very first evidence of ACKR3 expression in IBC cells. Thus, it provides the foundation for further characterization of the role of chemokine receptors in the progression of IBC disease and any other translational investigations focused on development of targeted therapies for this aggressive form of breast cancer.

Supplementary data to this article can be found online at http://dx.doi.org/10.1016/j.tranon.2015.07.002.

## Conflicts of interest

none

## Authors' contributions

RW characterized the properties of the FC-IBC02A cells in culture, determined expression and function of chemokine receptors in vitro, and carried out the shorter term in vivo studies; KT generated the cells stably expressing GFP and Luciferase, performed the long-term in vivo studies, and assembled a first draft of the manuscript; DJ participated to the generation of the GFP+ cells and performed initial intra-cardiac injections; SVF and MC isolated the FC-IBC02A cells, established the cultures, and provided relevant clinical data; AF generated the animal model of metastasis and participated to the design of the in vivo studies; OM conceived and designed the overall study, analyzed the data (with RW, KT, and AF), wrote the manuscript, and supervised/coordinated all phases of research. All authors have read and approved the final manuscript.

## Acknowledgments

The authors wish to thank Dr. Mark Penfold (ChemoCentryx) for the anti-ACKR3 antibody and CCX733, and the NIH (R01DA15014 to OM) and the PA Breast Cancer Coalition (Refunds for Research Grant to AF) for their support. RW was the recipient of a post-doctoral FIRC fellowship (2012-13).

## References

[1] Robertson FM, Bondy M, and Yang W, et al (2010). Inflammatory breast cancer: the disease, the biology, the treatment. *CA Cancer J Clin* **60**(6), 351–375.

[2] Kleer CG, van Golen KL, and Merajver SD (2000). Molecular biology of breast cancer metastasis. Inflammatory breast cancer: clinical syndrome and molecular determinants. *Breast Cancer Res* **2**(6), 423–429.

[3] Hance KW, Anderson WF, and Devesa SS, et al (2005). Trends in inflammatory breast carcinoma incidence and survival: the surveillance, epidemiology, and end results program at the National Cancer Institute. *J Natl Cancer Inst* **97**(13), 966–975.

[4] Dawood S and Cristofanilli M (2011). Inflammatory breast cancer: what progress have we made?*Oncology (Williston Park)* **25**(3), 264–270 [273].

[5] Ueno NT, Buzdar AU, and Singletary SE, et al (1997). Combined-modality treatment of inflammatory breast carcinoma: twenty years of experience at M. D. Anderson Cancer Center. *Cancer Chemother Pharmacol* **40**(4), 321–329.

[6] Low JA, Berman AW, and Steinberg SM, et al (2004). Long-term follow-up for locally advanced and inflammatory breast cancer patients treated with multimodality therapy. *J Clin Oncol* **22**(20), 4067–4074.

[7] Muller A, Homey B, and Soto H, et al (2001). Involvement of chemokine receptors in breast cancer metastasis. *Nature* **410**(6824), 50–56.

[8] Cabioglu N, Gong Y, and Islam R, et al (2007). Expression of growth factor and chemokine receptors: new insights in the biology of inflammatory breast cancer. *Ann Oncol* **18**(6), 1021–1029.

[9] Burger JA and Kipps TJ (2006). CXCR4: a key receptor in the crosstalk between tumor cells and their microenvironment. *Blood* **107**(5), 1761–1767.

[10] Liang Z, Wu T, and Lou H, et al (2004). Inhibition of breast cancer metastasis by selective synthetic polypeptide against CXCR4. *Cancer Res* **64**(12), 4302–4308.

[11] Salmaggi A, Maderna E, and Calatozzolo C, et al (2009). CXCL12, CXCR4 and CXCR7 expression in brain metastases. *Cancer Biol Ther* **8**(17), 1608–1614.

[12] Domanska UM, Kruizinga RC, and Nagengast WB, et al (2013). A review on CXCR4/CXCL12 axis in oncology: no place to hide. *Eur J Cancer* **49**(1), 219–230.

[13] Li YM, Pan Y, and Wei Y, et al (2004). Upregulation of CXCR4 is essential for HER2-mediated tumor metastasis. *Cancer Cell* **6**(5), 459–469.

[14] Bachelerie F, Graham GJ, and Locati M, et al (2014). New nomenclature for atypical chemokine receptors. *Nat Immunol* **15**(3), 207–208.

[15] Bachelerie F, Ben-Baruch A, and Burkhardt AM, et al (2014). International Union of Basic and Clinical Pharmacology. [corrected]. LXXXIX. Update on the extended family of chemokine receptors and introducing a new nomenclature for atypical chemokine receptors. *Pharmacol Rev* **66**(1), 1–79.

[16] Levoye A, Balabanian K, and Baleux F, et al (2009). CXCR7 heterodimerizes with CXCR4 and regulates CXCL12-mediated G protein signaling. *Blood* **113**(24), 6085–6093.

[17] Luker KE, Steele JM, and Mihalko LA, et al (2010). Constitutive and chemokine-dependent internalization and recycling of CXCR7 in breast cancer cells to degrade chemokine ligands. *Oncogene* **29**(32), 4599–4610.

[18] Busillo JM, Armando S, and Sengupta R, et al (2010). Site-specific phosphorylation of CXCR4 is dynamically regulated by multiple kinases and results in differential modulation of CXCR4 signaling. *J Biol Chem* **285**(10), 7805–7817.

[19] Fernandez SV, Robertson FM, and Pei J, et al (2013). Inflammatory breast cancer (IBC): clues for targeted therapies. *Breast Cancer Res Treat* **140**(1), 23–33.

[20] Liu Q, Russell MR, and Shahriari K, et al (2013). Interleukin-1beta promotes skeletal colonization and progression of metastatic prostate cancer cells with neuroendocrine features. *Cancer Res* **73**(11), 3297–3305.

[21] Russell MR, Liu Q, and Fatatis A (2010). Targeting the {alpha} receptor for platelet-derived growth factor as a primary or combination therapy in a preclinical model of prostate cancer skeletal metastasis. *Clin Cancer Res* **16**(20), 5002–5010.

[22] Dong HM, Liu G, and Hou YF, et al (2007). Dominant-negative E-cadherin inhibits the invasiveness of inflammatory breast cancer cells in vitro. *J Cancer Res Clin Oncol* **133**(2), 83–92.

[23] Kleer CG, van Golen KL, and Braun T, et al (2001). Persistent E-cadherin expression in inflammatory breast cancer. *Mod Pathol* **14**(5), 458–464.

[24] Tomlinson JS, Alpaugh ML, and Barsky SH (2001). An intact overexpressed E-cadherin/alpha, beta-catenin axis characterizes the lymphovascular emboli of inflammatory breast carcinoma. *Cancer Res* **61**(13), 5231–5241.

[25] Christiansen JJ and Rajasekaran AK (2006). Reassessing epithelial to mesenchymal transition as a prerequisite for carcinoma invasion and metastasis. *Cancer Res* **66**(17), 8319–8326.

[26] Moreno-Bueno G, Portillo F, and Cano A (2008). Transcriptional regulation of cell polarity in EMT and cancer. *Oncogene* **27**(55), 6958–6969.

[27] Mani SA, Guo W, and Liao MJ, et al (2008). The epithelial-mesenchymal transition generates cells with properties of stem cells. *Cell* **133**(4), 704–715.

[28] Sheridan C, Kishimoto H, and Fuchs RK, et al (2006). CD44+/CD24- breast cancer cells exhibit enhanced invasive properties: an early step necessary for metastasis. *Breast Cancer Res* **8**(5), R59.

[29] Abraham BK, Fritz P, and McClellan M, et al (2005). Prevalence of CD44+/CD24-/low cells in breast cancer may not be associated with clinical outcome but may favor distant metastasis. *Clin Cancer Res* **11**(3), 1154–1159.

[30] Bos PD, Nguyen DX, and Massague J (2010). Modeling metastasis in the mouse. *Curr Opin Pharmacol* **10**(5), 571–577.

[31] Liu KK and Dorovini-Zis K (2009). Regulation of CXCL12 and CXCR4 expression by human brain endothelial cells and their role in CD4+ and CD8+ T cell adhesion and transendothelial migration. *J Neuroimmunol* **215**(1-2), 49–64.

[32] Sun X, Cheng G, and Hao M, et al (2010). CXCL12 / CXCR4 / CXCR7 chemokine axis and cancer progression. *Cancer Metastasis Rev* **29**(4), 709–722.

[33] Miao Z, Luker KE, and Summers BC, et al (2007). CXCR7 (RDC1) promotes breast and lung tumor growth in vivo and is expressed on tumor-associated vasculature. *Proc Natl Acad Sci U S A* **104**(40), 15735–15740.

[34] Singh B, Cook KR, and Martin C, et al (2010). Evaluation of a CXCR4 antagonist in a xenograft mouse model of inflammatory breast cancer. *Clin Exp Metastasis* **27**(4), 233–240.

[35] Shimizu S, Brown M, and Sengupta R, et al (2011). CXCR7 protein expression in human adult brain and differentiated neurons. *PLoS One* **6**(5), e20680.

[36] Naumann U, Cameroni E, and Pruenster M, et al (2010). CXCR7 functions as a scavenger for CXCL12 and CXCL11. *PLoS One* **5**(2), e9175.

[37] Wojcechowskyj JA, Lee JY, and Seeholzer SH, et al (2011). Quantitative phosphoproteomics of CXCL12 (SDF-1) signaling. *PLoS One* **6**(9), e24918.

[38] Hatse S, Princen K, and Bridger G, et al (2002). Chemokine receptor inhibition by AMD3100 is strictly confined to CXCR4. *FEBS Lett* **527**(1-3), 255–262.

[39] Luker KE, Gupta M, and Steele JM, et al (2009). Imaging ligand-dependent activation of CXCR7. *Neoplasia* **11**(10), 1022–1035.

[40] Kakinuma T and Hwang ST (2006). Chemokines, chemokine receptors, and cancer metastasis. *J Leukoc Biol* **79**(4), 639–651.

[41] Lee BC, Lee TH, and Avraham S, et al (2004). Involvement of the chemokine receptor CXCR4 and its ligand stromal cell-derived factor 1alpha in breast cancer cell migration through human brain microvascular endothelial cells. *Mol Cancer Res* **2**(6), 327–338.

[42] Furusato B, Mohamed A, and Uhlen M, et al (2010). CXCR4 and cancer. *Pathol Int* **60**(7), 497–505.

[43] Zeelenberg IS, Ruuls-Van Stalle L, and Roos E (2003). The chemokine receptor CXCR4 is required for outgrowth of colon carcinoma micrometastases. *Cancer Res* **63**(13), 3833–3839.